A comparison between excess barium and barite as indicators of carbon export

Meagan Eagle and Adina Paytan
Department of Geological and Environmental Sciences, Stanford University, Stanford, California, USA

Kevin R. Arrigo and Gert van Dijken
Department of Geophysics, Stanford University, Stanford, California, USA

Richard W. Murray
Department of Earth Sciences, Boston University, Boston, Massachusetts, USA

Received 2 April 2002; revised 6 November 2002; accepted 3 December 2002; published 27 March 2003.

[1] Since *Dymond et al.* [1992] proposed the paleoproductivity algorithm based on "Bio-Ba," which relies on a strong correlation between Ba and organic carbon fluxes in sediment traps, this proxy has been applied in many paleoproductivity studies. Barite, the main carrier of particulate barium in the water column and the phase associated with carbon export, has also been suggested as a reliable paleoproductivity proxy in some locations. We demonstrate that Ba_{excess} (total barium minus the fraction associated with terrigenous material) frequently overestimates Ba_{barite} (barium associated with the mineral barite), most likely due to the inclusion of barium from phases other than barite and terrigenous silicates (e.g., carbonate, organic matter, opal, Fe-Mn oxides, and hydroxides). A comparison between overlying oceanic carbon export and carbon export derived from Ba_{excess} shows that the *Dymond et al.* [1992] algorithm frequently underestimates carbon export but is still a useful carbon export indicator if all caveats are considered before the algorithm is applied. Ba_{barite} accumulation rates from a wide range of core top sediments from different oceanic settings are highly correlated to surface ocean ^{14}C and Chlorophyll *a* measurements of primary production. This relationship varies by ocean basin, but with the application of the appropriate f ratio to ^{14}C and Chlorophyll *a* primary production estimates, the plot of Ba_{barite} accumulation and carbon export for the equatorial Pacific, Atlantic, and Southern Ocean converges to a global relationship that can be used to reconstruct paleo carbon export. *INDEX TERMS:* 3022 Marine Geology and Geophysics: Marine sediments—processes and transport; 4267 Oceanography: General: Paleoceanography; 4825 Oceanography: Biological and Chemical: Geochemistry; *KEYWORDS:* paleoproductivity, barite, export production, excess barium, marine sediments

Citation: Eagle, M., A. Paytan, K. R. Arrigo, G. van Dijken, and R. W. Murray, A comparison between excess barium and barite as indicators of carbon export, *Paleoceanography*, *18*(1), 1021, doi:10.1029/2002PA000793, 2003.

1. Introduction

[2] Marine barite ($BaSO_4$) has long been associated with decaying organic matter [*Dehairs et al.*, 1980; *Bishop*, 1988] and has recently been shown to precipitate during phytoplankton decay [*Ganeshram et al.*, 2002]. This results in a positive correlation between "Bio-Ba" and organic carbon fluxes as observed in sediment traps and filtered particulate matter [*Dehairs et al.*, 1990; *Dymond et al.*, 1992; *Francois et al.*, 1995; *Dymond and Collier*, 1996]. Based on this relationship in sediment traps, *Dymond et al.* [1992] predicted a positive correlation between the accumulation of barium (Ba) that is not of terrigenous origin (e.g., "Bio-Ba," hereafter referred to as Ba_{excess}) and carbon export. Ba_{excess} in this relation is presumed to be the fraction of sedimentary Ba associated with the carbon export flux.

[3] Barite is a major carrier of particulate Ba in the water column and has been implicated in several studies as the particulate Ba phase directly related to marine carbon export flux [*Bishop*, 1988; *Dymond et al.*, 1992]. Indeed, the algorithm suggested by *Dymond et al.* [1992] relies on the predictable formation of barite in association with sinking organic carbon. As stated by *Dymond et al.* [1992, p. 172], "The usefulness of C_{org}/Ba relationships as paleoproductivity indicators depends on whether the syngenetically formed barite is the predominant contribution to the barium flux..." Barium, however, is contained in other phases, some of which are also biogenically related (e.g., organic matter, biogenic silica and biogenic carbonate), and others that are not directly related to carbon export (e.g., terrigenous silicates, Fe-Mn oxides and hydroxides). The nonbarite phases which are included in Ba_{excess} would not necessarily yield a predictable global C_{org}/Ba_{excess} relationship as found by *Dymond et al.* [1992] because the ratio of organic carbon to these other biologically related Ba phases varies spatially in the ocean, and factors controlling Ba incorporation into Fe-Mn oxides and hydroxides are not directly biologically mediated. Moreover, it must also be noted that the *Dymond et al.* [1992] algorithm is based

0883-8305/03/2002PA000793$12.00

predominantly on sediment trap work and does not take into account post depositional changes in particulate barium associations, therefore caution must be used in the application of the Ba_{excess} paleoproductivity proxy to sediments, as emphasized by *Dymond et al.* [1992].

[4] Despite these potential complications, Ba_{excess} has been used in many studies, to infer paleoproductivity [*Schmitz*, 1987; *Rutsch et al.*, 1995; *Dean et al.*, 1997; *Nürnberg et al.*, 1997; *Bonn et al.*, 1998; *Bains et al.*, 2000]. Ba_{excess} is determined from the total Ba concentration in the sediment minus the Ba associated with terrigenous material, which is calculated from total Al and normalization to a constant Ba/Al ratio (typically Ba/Al of average shale, 0.0075, see preceding references). This calculation assumes that (1) all sedimentary particulate Ba besides the fraction associated with terrigenous aluminosilicates is predictably related to carbon export; (2) all of the Al is associated with terrigenous material; (3) and the Ba/Al ratio used is in fact representative of each sample's terrigenous component and is constant in space and time. If the above assumptions are correct and we accept the water column relationships for sedimentary barium, then terrigenous Ba concentrations can indeed be calculated from total Al in the sample and subtraction of this component from total Ba will yield an accurate estimate of biogenically related Ba and carbon export.

[5] Previous research on the relationship between productivity and Ba in the water column and sediment suggests, however, that the above assumptions may not always hold. Sediment trap and particulate matter studies have shown that although barite is the major Ba carrier in water column bulk sinking particulate matter, Ba is also present in biogenic SiO_2, $CaCO_3$, organic matter and aluminosilicates [*Dehairs et al.*, 1980; *Collier and Edmond*, 1984]. In marine sediments, some Ba may also be associated with Fe-Mn oxides and hydroxides [*Dymond et al.*, 1992; *Schroeder et al.*, 1997; *McManus et al.*, 1998]. Quantitative estimates of the fraction of Ba_{excess} associated with all of these phases and how these fractions vary in different sedimentary settings have yet to be published, although various investigators have used a variety of selective leaching procedures to determine Ba associations [*Wefer et al.*, 1982; *Dymond et al.*, 1992; *Schenau et al.*, 2001; *Eagle and Paytan*, 2001]. Collectively, these studies indicate that in many regimes, what is loosely referred to in the literature as "Bio Ba" is not necessarily associated with the predictably related productivity component of Ba (e.g., barite), suggesting that condition (1) above is not always met. In other words, Ba associated with components such as Fe-Mn oxides and hydroxides is also included in Ba_{excess} and is unlikely to be related to carbon export.

[6] An additional source of error may be variability in the Ba/Al ratios of terrigenous material. *Klump et al.* [2000] found that Ba/Al for the Chilean margin surface sediments varied considerably (0.0028 to 0.0239), and concluded that Ba_{excess} calculations in samples with a high terrigenous component may be sensitive to changes in this ratio. This variation appears to be more extreme than the end-member ratios (0.0045 to 0.01) suggested by *Dymond et al.* [1992], and from the average (0.0075) used in most previous applications of Ba_{excess} for paleoproductivity reconstruction. Uncertainties arising from terrigenous Ba correction using total Al can, in some cases, be accounted for by applying a similar Ti normalization in locations that are not influenced by significant volcanic input [*Murray and Leinen*, 1993; *Dymond and Collier*, 1996; *Schroeder et al.*, 1997; *Murray et al.*, 2000]. In addition, the nonterrigenous Al component of diatom tests, the Al associated with other sedimentary phases [*Van Bennekom et al.*, 1989; *Van Capellen et al.*, 2001] and Al adsorbed onto sinking particles [*Murray et al.*, 1993; *Murray and Leinen*, 1996] may affect Ba_{excess} values. These observations indicate that assumptions (2) and (3) above also are not universally applicable.

[7] To prevent some of these potential complications, *Paytan et al.* [1996] proposed an algorithm for paleoproductivity reconstruction in the equatorial Pacific based directly on barite accumulation in core top sediments. In that study, as that by *Dymond et al.* [1992], the applicability of the proxy relies on the observation that barite forms and accumulates in proportion to organic matter decomposition in the water column. In addition, barite shows promise as a paleoproductivity proxy because it is a highly refractory mineral with preservation as high as 30% in oxic sediments [*Dymond et al.*, 1992; *Paytan and Kastner*, 1996]. The barite accumulation rate in oxic sediments could therefore be a superior proxy for estimating paleo carbon export if the processes controlling barite formation and preservation are known and operate globally in the ocean. The applicability of this proxy to oceanic settings other than the equatorial Pacific has yet to be tested.

[8] To test the robustness of the Ba_{excess} and barite accumulation proxies in light of the assumptions stated above, we (1) compared the sedimentary Ba fraction included in Ba_{excess} to the Ba fraction directly derived from barite, (2) compared carbon export calculated using core top Ba_{excess} values and the *Dymond et al.* [1992] algorithm to measured oceanic carbon export flux, and (3) correlated barite accumulation rates in core tops from throughout the global oceans to ^{14}C and Chlorophyll *a* (Chl *a*) primary production and carbon export.

2. Methods

[9] Core top samples, from the Pacific, Atlantic and Southern Oceans, were selected to represent different concentrations of Ba_{total} and correspond to a variety of sediment types, including calcareous and siliceous oozes, and contain varying amounts of terrigenous input (Table 1). Most samples used are from the upper 10 cm of the sedimentary column.

2.1. Barite Separation

[10] Barite was separated from the sediment using a sequential leaching procedure that includes reaction with acetic acid, sodium hypochlorite, hydroxylamine, and an HF-HNO_3 mixture (Table 2) [*Collier and Edmond*, 1984; *Paytan*, 1996; *Paytan et al.*, 1996]. During barite extraction, each of the leaching steps targets a major (operationally defined) sedimentary fraction, leaving a final residue composed of barite and a few other refractory minerals. The

Table 1. Sample Locations and Descriptions

Sample	Latitude	Longitude	Depth, m	Core Description	Sample Repository
NBP 9802 St. 3 0–5 cm	−66.128	−169.490	3222	Diatomaceous ooze with IRD and Mn nodules	LDEO
NBP 9802 St. 4 0–5 cm	−64.197	−170.081	2685	Diatomaceous ooze	LDEO
NBP 9802 St. 5 0–5 cm	−63.166	−169.852	2861	Diatomaceous ooze	LDEO
NBP 9802 St. 6 0–5 cm	−61.875	−169.972	3243	Diatomaceous ooze	LDEO
NBP 9802 St. 7 0–5 cm	−60.284	−170.023	3995	Diatomaceous and carbonate ooze	LDEO
NBP 9802 St. 8 0–5 cm	−58.688	−169.979	4324	Diatomaceous and carbonate ooze	LDEO
NBP 9802 St. 9 0–5 cm	−56.881	−170.171	4968	Clay with some diatomaceous ooze	LDEO
Pluto III 25BC 5–7 cm	8.790	−103.988	3180	Siliceous ooze	OSU
PLDS 81 0–5 cm	1.028	−124.622	4773	Calcareous, biogenic mud or ooze, sandy	SIO
PLDS 107 0–5, 15–20 cm	6.157	−138.277	4849	Calcareous, biogenic mud or ooze, sandy	SIO
JGOFS TT013-143MC 0–5 cm	8.920	−139.850	4992	Siliceous ooze	URI
JGOFS TT013-104MC 0–5 cm	5.780	−140.130	4413	Calcareous ooze	URI
JGOFS TT013-113MC 0–5 cm	4.040	−139.850	4431	Calcareous ooze	URI
JGOFS TT013-82MC 0–5 cm	2.500	−140.920	4412	Calcareous ooze	URI
JGOFS TT013-88MC 0–5 cm	1.000	−139.750	4315	Calcareous ooze	URI
JGOFS TT013-69MC 0–5 cm	0.100	−139.720	4301	Calcareous ooze	URI
JGOFS TT013-20MC 0–5 cm	−1.870	−139.700	4376	Calcareous ooze	URI
JGOFS TT013-35MC 0–5 cm	−4.970	−139.730	4263	Calcareous ooze	URI
JGOFS TT013-06MC 0–5 cm	−12.000	−134.950	4282	Siliceous ooze	URI
Manop K7905-21BC 0–5 cm	1.053	−138.947	4442	Calcareous, nannofossil ooze	OSU
TNO57-10 0–5 cm	−47.087	5.92	4398	Siliceous ooze with clay, foraminifera bearing	FSU
TNO57-13 0–5 cm	−53.175	5.127	2851	Diatomaceous ooze	FSU
PS 2489-4 0–5 cm	−42.883	8.968	3795	Calcareous ooze	Bremen
PS 2493-3 0–5 cm	−42.892	−6.022	4174	Calcareous ooze with siliceous component	Bremen
PS 2498-2 0–5 cm	−44.512	−14.228	3782	Calcareous ooze	Bremen
PS 2499-1 0–5 cm	−46.512	−15.333	3176	Calcareous ooze with siliceous component	Bremen
ERDC 88 0–9 cm	−0.480	155.868	1924	Calcareous, foraminiferal mud or ooze, sandy	SIO
ERDC 125 5–10 cm	−0.003	160.998	3368	Calcareous, biogenic mud or ooze, sandy	SIO
RC-24-08GC 11–13 cm	−1.337	−11.900	3882	Calcareous, foraminiferal ooze, sandy	LDEO
VM-30-41IL 11–13 cm	0.217	−23.067	3874	Foraminiferal ooze	LDEO
W7706-44K 10–15, 15–20 cm	−11.410	−78.230	580	Calcareous, foraminiferal ooze, minor sandy terrigenous component	OSU
INMD 106 10–15, 15–20 cm	2.732	−20.938	4702	Terrigenous mud or ooze with some calcareous foraminifera and nannofossils	SIO

Table 2. Barite Separation Sequential Leaching Procedure[a]

	Procedure Steps
1	Weigh ~10 grams dry sediment
2	Remove carbonates with 4 N ACETIC ACID (room temperature, ~12 hours)
3	Wash 3 times with DI water (repeat after each step)
4	Remove organic matter in 5% sodium hypochlorite (50°C, ~12 hours)
5	Remove Fe-Mn oxyhydroxides with 0.2 N hydroxylamine in 25% acetic acid (by volume) (80°C, ~12 hours)
6	Digest in 1:2 40% hydrofluric acid:1 N nitric acid (room temperature, ~12 hours)
7	Digest in 1:1 40% hydrofluric acid:1 N nitric acid (room temperature, ~12 hours)
8	Digest in 2:1 40% hydrofluric acid:1 N nitric acid (room temperature, ~12 hours)
9	Rinse residue in saturated $AlCl_3$ in 0.1N HNO_3 to remove fluorides (90°C, 1 hour)
10	Weigh residue and check purity with SEM or bulk dissolution of residue

[a]After *Paytan* [1996].

yield of this extraction (~95%) was determined by (1) submitting a reagent-grade barite sample to the sequential leaching procedure, (2) adding a known amount of natural marine barite (previously separated from marine sediments) to a barite free artificial sediment mix (65% $CaCO_3$, 20% kaolinite, 10% opal and 5% quartz) and subjecting this mixture to the sequential leaching procedure, and (3) adding known amounts of natural marine barite to a bulk core top sediment sample and retrieving the amount added after the extraction procedure (standard additions). In the first recovery experiment described above, the reagent grade barite crystals are smaller than natural barite crystals found in sediments (0.25–1 μm, compared to 1–5 μm for sedimentary barite) and were treated without a sediment matrix. This makes the barite in this experiment more susceptible to dissolution and mechanical loss (larger surface area-to-volume ratio and reagent reacts only with barite) than barite in sediment samples, so the percent recovery of this experiment is considered a minimum for the sequential leaching procedure. The barite used in the other two recovery tests was previously separated from marine sediment. We recognize that this barite might be considered ''insoluble'' to the sequential leaching procedure and so guarantee high recovery. However, given the consistently high recoveries in all three tests, and the close agreement between Ba_{barite} and Ba_{excess} in some sediments (see Table 3), we conclude that there is minimal dissolution of barite during the sequential leaching procedure. As a further check, in the pure barite sample treated without a sediment matrix, we analyzed the leachates from each step of the sequential dissolution for Ba, and found that only 15% of the total barite lost (which was <5% of original barite) had dissolved (e.g., was found in the leachate). Thus mechanical loss of the very small barite crystals during decanting and/or filtration accounted for the majority of the barite loss in the sample treated without a sediment matrix. While such mechanical loss is expected to be much less in sediment samples, this is important because the amount of barite lost may represent a relatively larger fraction of the total barite in samples with low wt% barite.

[11] The insoluble residue of the sequential leaching procedure is examined under a scanning electron microscope (SEM) to determine barite content. Rutile and anatase (TiO_2) are the most common minerals other than barite in the residue, and it is easy to differentiate them from barite by crystal size and shape (Figure 1). The barite content in the residue (% of the total residue) was determined using a backscattered electron imagining (BEI) detector mounted on the SEM and the EDX™ Image/Mapping (version 3.3) program. Ba_{barite} concentrations of the residue were calculated by first determining the total area of residue in view with the EDX™ Image/Mapping program. Then the percent area of the view occupied by barite was illuminated with the BEI detector, under which barite was the only illuminated mineral in the residue. This procedure was completed five times per sample and averaged to determine Ba_{barite} concentrations. Our detection limit in this procedure is about 20 μg barite. This is less than 20 ppm Ba_{barite} for all samples used here. For comparison, we also dissolved (bulk dissolution method, see below) the residue of several samples and measured total Ba (equal to Ba_{barite}); agreement with the SEM method was typically within ±10%. SEM analysis tended to underestimate Ba_{barite} compared to bulk dissolution of the residue. For example, at NBP 9802 St. 3 Ba_{barite} was 8% less in SEM analysis than the bulk dissolution of residue, St. 5 and 6 were both below the detection limits in both methods, and K7905-21 SEM estimates were 6% less than bulk dissolution.

2.2. Bulk Dissolution

[12] For bulk dissolution, samples were dissolved using a hot HF-HNO_3-H_2O_2 mixture [*Collier and Edmond*, 1984]. The total Ba (Ba_{total}) and total Al (Al_{total}) concentrations were measured with a TJA Iris Advantage/1000 inductively coupled argon plasma (ICAP) Spectrometer fitted with a solid state charge injection device (CID) detector to analyze multiple elements concurrently. Analytical precision was monitored with internal standards and remained <1% throughout the analysis period. Leachate blanks and total procedure blanks contributed <0.01% of total Ba in all samples. Duplicate samples were analyzed to monitor natural variability between splits of the same sample and were within 10% of each other. Ba_{excess} concentrations were calculated as

$$[Ba_{excess}]_{ppm} = [Ba_{total}]_{ppm} - \left(Ba/Al_{terrigenous}\right) \times [Al_{total}]_{ppm}, \quad (1)$$

where the Ba/Al ratio is presumed to be representative of terrigenous input to the ocean and serves as a correction factor for subtracting Ba associated with terrigenous inputs.

We have compared two widely used Ba/Al ratios (0.0045 and 0.0075) to demonstrate the range of Ba_{excess} that could be derived for each sample using these typical values. However, it must be emphasized that the actual range of Ba/Al observed in the terrigenous component of marine sediments is significantly larger [*Klump et al.*, 2000].

2.3. Productivity Estimates

[13] New production (e.g., carbon export) was calculated from Ba_{excess} with the *Dymond et al.* [1992] algorithm:

$$P_{new} = \left(\frac{F_{Ba}0.171Ba^{2.218}z^{0.476-0.00478Ba}}{2056}\right)^{1.504} \quad (2)$$

Where F_{Ba} is the accumulation rate of Ba_{excess} (corrected for Ba_{excess} preservation in sediments as suggested by *Dymond et al.* [1992]), Ba is the concentration of barium at 1700 m water depth, and z is the water depth. Dissolved Ba concentrations were taken from the Geochemical Ocean Sections Study (GEOSECS) stations nearest to core locations and at a depth closest to 1700 m [*GEOSECS*, 1987]. Given the small difference between Ba_{excess} calculated with the two terrigenous Ba/Al ratios for these open ocean samples (discussed below), we used only Ba_{excess} calculated with a Ba/Al of 0.0075 for comparison with water column estimates of carbon export.

[14] Surface ocean primary productivity for the majority of the samples used here was obtained from multiple year averages of direct measurements of in situ ^{14}C incorporation or Chl *a* measurements; sources are included in Table 3. All other primary productivity estimates (when direct measurements were unattainable or were measured infrequently) are based on a numerical algorithm [*Arrigo et al.*, 1998] that was used to estimate daily primary production (g C m^{-2} d^{-1}) from Chl *a* fields obtained from sea-viewing wide field-of-view sensor (SeaWiFS) measurements of ocean color between 1997 and 2001. The algorithm uses Chl *a* concentration, temperature, mixed layer depth, and diurnal changes in spectral irradiance to calculate primary production. SeaWiFS data were obtained from the Goddard Earth Sciences Data and Information Services Center, DAAC. Chl *a* concentrations were derived from monthly averaged SeaWiFS Level 3 data (9 km resolution, reprocessing version 4) and processed using the NASA SeaDAS image processing software and the OC4v4 algorithm. Mixed layer depths are from *Kara et al.* [2002]. Diurnal variation in spectral irradiance at each station was determined from the clear sky model of *Gregg and Carder* [1990]. Clear sky irradiance was corrected for fractional cloud cover, determined from NCEP/NCAR data, according to the equation of *Dobson and Smith* [1988]. Sea level pressure, wind speed, and sea surface temperature used as input to the algorithm were obtained from COADS [*Slutz et al.*, 1985]; relative humidity was from *da Silva et al.* [1994] and precipitable water from NCEP/NCAR [*Kalnay et al.*, 1996].

[15] Although direct primary productivity estimates for one year (1997–1998, ASOPES JGOFS study) from the Southern ocean transect across 170° W (NBP 9802 samples) are available [*Nelson et al.*, 2002; *Buesseler et al.*, 2003; *Hiscock et al.*, 2003], we used the numerical algorithm model productivity, described above, for these sites. The model represents several years of data and may be more representative of the annual mean, considering the spiky and patchy nature of phytoplankton blooms in this area that make annual estimates of productivity difficult to extrapolate from infrequent shipboard measurements. The measured productivity in 1997–1998 in all NBP 9802 stations is higher then the model derived values.

[16] Relatively few multiyear averages of direct new production (equivalent to carbon export here) measurements are available, so we used primary productivity measurements (as described above) and applied an appropriate f ratio to estimate carbon export fluxes. Water column carbon export was calculated by multiplying the primary productivity values (derived from ^{14}C incorporation or Chl *a*) with the appropriate f ratios (Table 3), allowing results to be compared with carbon flux (or P_{new} values) calculated from Ba_{excess} and the *Dymond et al.* [1992] algorithm. An f ratio of 0.15 was used for the tropical Pacific [*Pena et al.*, 1992; *McCarthy et al.*, 1996; *Aufdenkampe et al.*, 2001], 0.5 for the Southern Ocean [*Metzler et al.*, 1997], 0.64 for south of the Antarctic Circumpolar Current [*Buesseler et al.*, 2003], and 0.05 for the Atlantic [*Wollast and Chou*, 2001].

2.4. Mass Accumulation Rates

[17] Mass accumulation rates for most of our samples have been previously published. Mass accumulation rates were determined by $^{230}Thorium_{ex}$ for NBP 9802 [*Chase*, 2001] and PS cores [*Nürnberg*, 1995], thus accounting for potential sediment focusing; by C^{14} dates for PLDS, ERDC [*Berger and Killingsley*, 1982] and TT013 cores [*DeMaster and Pope*, 1994]; and by O^{18} stratigraphy for TNO57 (C. Charles, personal communication, 1999). For the remaining samples, dry bulk density (DBD) was estimated with wt% $CaCO_3$, utilizing equation (5) from *Snoeckx and Rea* [1994]. MAR were calculated for W7706 with wt% $CaCO_3$ and sedimentation rates from *Krissek et al.* [1980], and for RC-24 and VM 30 with wt% $CaCO_3$ from *Curry and Lohmann* [1990] and sedimentation rates from *Mix et al.* [1986].

3. Results and Discussion

3.1. Comparison Between Ba_{excess} and Ba_{barite}

[18] For most samples used in this study, Ba_{excess} values, calculated using either of the two representative Ba/Al ratios (Table 3; Figure 2), overestimate the Ba fraction associated with barite. This overestimate ranges from as little as a few percent in some sediments to 100% in sediments with low total Ba. In the most extreme case, 3800 ppm Ba_{excess} was measured in one sample despite there being no observed barite (Pluto III). The percent Ba_{barite}/Ba_{excess} (Table 3) is an approximation of how much Ba_{excess} exceeds Ba_{barite}. In general, no Ba_{barite} is observed in sediments with low total Ba and Ba_{excess} between 10–100 ppm (Ba_{barite}/Ba_{excess} is 0%, see sample RC-24 for example). In these sediments, it is clear that Ba_{excess} does not correspond to Ba_{barite}. However, even in some sediments with high total Ba concentrations (1000–6000 ppm, Pluto III, NBP 9802, and TNO57-13), Ba_{excess} may not always be a good measure of Ba_{barite}. In these samples, only a fraction of Ba_{excess} is associated with barite (0–70%).

Table 3. Ba_{barite} and Ba_{excess} Comparisons, MAR and Productivity

Sample	Ba_{barite},[a] ppm	Ba_{total},[b] ppm	Al_{total},[b] ppm	Ba_{excess},[b] ppm Ba/Al = 0.0075/0.0045	Ba_{barite}/Ba_{excess}, % Ba/Al = 0.0075/0.0045	MAR,[c] g m^{-2} yr^{-1}	Ba_{barite} AR, μg m^{-2} yr^{-1}	Ba_{excess} AR, μg cm^{-2} yr^{-1} 0.0075/0.0045	P_{new}, [after *Dymond et al.*, 1992] g C m^{-2} y^{-1} 0.0075/0.0045	Export Production,[d] g C m^{-2} y^{-1}	f Ratio[e]
NBP 9802 St. 3 0–5 cm	3953	6097	38359	5809/5924	68/67	3.1	12.2	17.9/18.3	51/52	32	0.64
NBP 9802 St. 3 0–5 cm (duplicate)	4272	5747	39133	5453/5571	78/77	3.1	13.2	16.9/17.2	46/48	32	0.64
NBP 9802 St. 4 0–5 cm	<20	1597	3108	1574/1583	0/0	7.4	0.0	11.6/11.7	19/19	15	0.50
NBP 9802 St. 5 0–5 cm	<20	1526	2150	1510/1516	1/1	10.6	0.2	16.1/16.1	27/27	15	0.50
NBP 9802 St. 6 0–5 cm	85	832	691	827/829	10/10	20.1	1.7	16.6/16.6	23/23	13	0.50
NBP 9802 St. 7 0–5 cm	1070	1540	5663	1498/1515	71/71	5.6	6.0	8.4/8.5	13/13	13	0.50
NBP 9802 St. 8 0–5 cm	1452	2351	22023	2185/2251	66/64	3.5	5.1	7.7/8.0	20/20	16	0.50
NBP 9802 St. 9 0–5 cm	535	1604	55542	1188/1354	45/39	2.4	1.3	2.8/3.2	5/6	14	0.50
Pluto III 25BC 5–7 cm	<20	4031	40273	3729/3850	0/0	7.2	0.0	26.8/27.7	41/43	19	0.15
PLDS 81 0–5 cm	812	4172	8126	4111/4135	20/20	5.2	4.2	21.4/21.5	31/31	25	0.15
PLDS 107 0–5 cm	1000	3049	29935	2825/2915	35/34	3.4	3.4	9.6/9.9	11/12	25	0.15
PLDS 107 15–20 cm	1294	2001	17342	1871/1923	69/67	3.4	4.4	6.4/6.5	6/6	25	0.15
JGOFS TT013-143MC 0–5 cm	2120	4339[f]	61844[f]	3875/4061	55/49	1.7	3.6	6.6/6.9	9/9	23	0.15
JGOFS TT013-104MC 0–5 cm	1000	1382[f]	6451[f]	1334/1353	75/72	12.8	12.8	17.1/17.3	16/17	29	0.15
JGOFS TT013-113MC 0–5 cm	1060	1929[f]	5236[f]	1890/1906	56/55	12.3	13.0	23.2/23.4	26/27	31	0.15
JGOFS TT013-82MC 0–5 cm	1420	1807[f]	4066[f]	1776/1788	80/79	9.5	13.5	16.9/17.0	18/18	34	0.15
JGOFS TT013-88MC 0–5 cm	1590	2108[f]	4592[f]	2073/2087	77/75	14.7	23.4	30.5/30.7	38/38	44	0.15
JGOFS TT013-69MC 0–5 cm	1530	1702[f]	3633[f]	1674/1685	91/90	15.2	23.3	25.5/25.6	28/29	50	0.15
JGOFS TT013-20MC 0–5 cm	767	1361[f]	2720[f]	1341/1349	57/56	18.6	14.3	24.9/25.1	26/26	39	0.15
JGOFS TT013-35MC 0–5 cm	295	967[a]	2449[a]	949/956	31/30	13.5	4.0	12.8/12.9	10/11	23	0.15
JGOFS TT013-06MC 0–5 cm	59	1988[f]	20232[f]	1836/1897	3/3	1.7	0.1	3.1/3.2	3/3	14	0.15
Manop K7905-21BC 0–5 cm	1166	2204	4164	2173/2185	54/53	14.7	17.1	31.9/32.1	40/41	44	0.15
TNO57-10 0–5 cm	1411	2856	35485	2590/2696	54/52	10.0	14.1	25.9/27.0	65/69	30	0.50
TNO57-13 0–5 cm	35	1247	8197	1186/1211	3/3	30.0	1.1	35.6/36.3	74/77	9	0.50

Table 3. (continued)

Sample	Ba_{barite},[a] ppm	Ba_{total},[b] ppm	Al_{total},[b] ppm	Ba_{excess},[b] ppm Ba/Al = 0.0075/0.0045	Ba_{barite}/Ba_{excess}, % Ba/Al = 0.0075/0.0045	MAR,[c] g m^{-2} yr^{-1}	Ba_{barite} AR, μg m^{-2} yr^{-1}	Ba_{excess} AR, μg cm^{-2} yr^{-1} 0.0075/0.0045	P_{new}, [after *Dymond et al.*, 1992] g C m^{-2} y^{-1} 0.0075/0.0045	Export Production,[d] g C m^{-2} y^{-1}	f Ratio[e]
PS 2489-4 0–5 cm	<20	205[g]	2000[g]	190/196	3/3	92.7	0.6	17.6/18.2	20/21	7	0.50
PS 2493-3 0–5 cm	41	994[g]	12400[g]	901/938	5/4	24.2	1.0	22.0/22.7	39/41	12	0.50
PS 2498-2 0–5 cm	201	217[g]	2000[g]	202/208	100/97	60.0	12.1	12.2/12.5	13/13	25	0.50
PS 2499-1 0–5 cm	649	574[g]	6200[g]	528/546	123/119	23.0	14.9	12.2/12.5	16/17	30	0.50
ERDC 88 0–9 cm	270	361	3367	335/346	81/78	8.0	2.2	2.7/2.8	1/1	16	0.15
ERDC 125 5–10 cm	51	665	6295	617/636	8/8	14.5	0.7	9.0/9.2	5/5	16	0.15
ERDC 125 5–10 cm (Duplicate)	51	662	6085	616/634	8/8	14.5	0.7	8.9/9.2	5/5	16	0.15
RC-24-08GGG 11–13 cm	<20	112	1454	101/106	0/0	54.8	0.0	5.6/5.8	2/2	10	0.05
VM-30-41IL 11–13 cm	100	119	5085	81/96	124/104	17.3	1.7	1.4/1.7	0.3/0.4	9	0.05
W7706-44K 10–15 cm	73	263	24663	78/152	94/48	90.1	6.6	7.0/13.7	3/9	90	0.15
W7706-44K 15–20 cm	75	250	29208	31/119	241/63	89.5	6.7	2.8/10.6	1/6	90	0.15
INMD 106 10–15 cm	<20	133	17911	−2/52	0/0	15.0	0.0	0.0/0.8	0.0/0.1	4	0.05
INMD 106 10–15 cm (Duplicate)	<20	136	20264	−16/45	0/0	15.0	0.0	−0.2/0.7	0.0/0.1	4	0.05
INMD 106 15–20 cm	<20	152	19745	4/64	0/0	15.0	0.0	0.1/1.0	0.0/0.2	4	0.05
INMD 106 15–20 cm (Duplicate)	<20	192	22620	22/90	0/0	15.0	0.0	0.3/1.3	0.0/0.3	4	0.05

[a]Sequential leaching barite separation (see section 2.1), minimum detection of 20 μg barite.

[b]Bulk dissolution (see section 2.2).

[c]Mass accumulation rates were determined by $^{230}Thorium_{ex}$ for NBP 9802 cores [*Chase*, 2001]; by C^{14} dates for PLDS 81 and 107 and ERDC 88 and 125 [*Berger and Killingsley*, 1982]; by C^{14} dates for TT013 (and K7905) samples [*DeMaster and Pope*, 1994]; by O^{18} stratigraphy for TNO57 (personal communication, Christopher Charles); and by $^{230}Thorium_{ex}$ for PS samples [*Nürnberg*, 1995]. For the remaining samples, dry bulk density (DBD) was estimated with wt% $CaCO_3$, utilizing equation (5) from [*Snoeckx and Rea*, 1994]. MARs were determined by multiplying sediment AR with DBD. Wt% $CaCO_3$ and sedimentation rates for W7706 by *Krissek et al.* [1980]; and wt% $CaCO_3$ [*Curry and Lohmann*, 1990] and sedimentation rates [*Mix et al.*, 1986] for RC-24 and VM 30.

[d]Productivity values for TT013, PLDS and ERDC samples are from [*Paytan et al.*, 1996]; for TNO57 and PS samples provided by O. Holm-Hansen (personal communication, 2002) based on a 20 year compilation of chlorophyll data for the region and production per chlorophyll unit; W7706 provided by R. Barber (personal communication, 2002) based on chlorophyll data; and for all other samples productivities are based on satellite measurements of Chl a. Appropriate f ratios have been applied to primary productivity to estimate export production. See section 2.3 for further discussion.

[e]An f ratio of 0.15 was used for the tropical Pacific [*Pena et al.*, 1992; *McCarthy et al.*, 1996; *Aufdenkampe et al.*, 2001], 0.5 for the Southern Ocean [*Metzler et al.*, 1997], 0.64 for south of the Antarctic Circumpolar Current [*Buesseler et al.*, 2003], and 0.05 for the Atlantic [*Wollast and Chou*, 2001].

[f]Bulk dissolution Ba_{total} and Al_{total} from *Schroeder et al.* [1997] and *Murray et al.* [2000].

[g]Bulk dissolution Ba_{total} and Al_{total} from *Nürnberg* [1995].

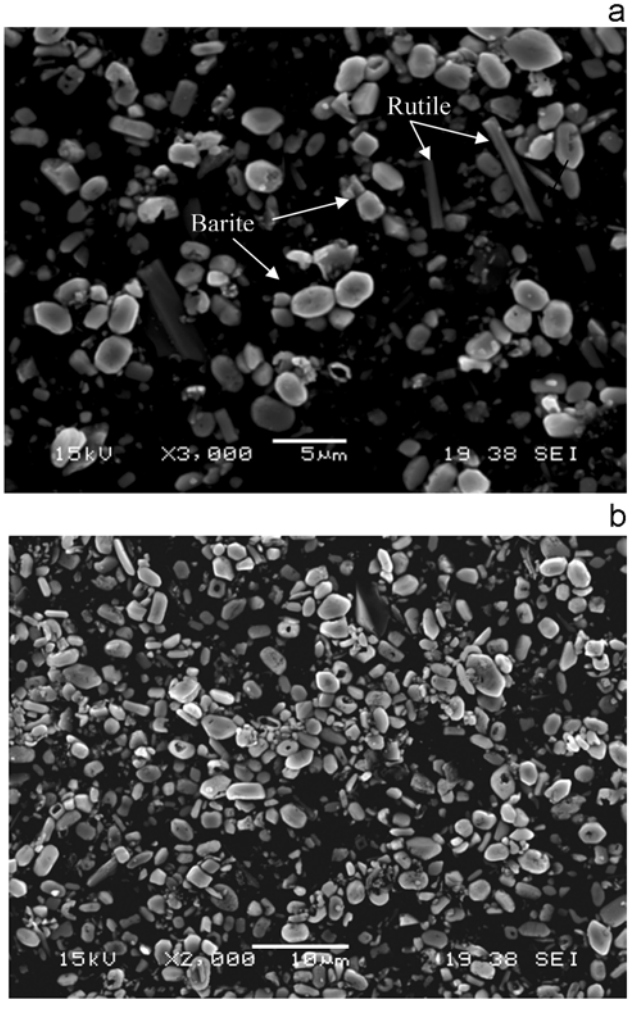

Figure 1. SEM images of the insoluble residue of barite separation sequential leaching procedure. (a) 1–3 μm round and elliptical barite crystals from NBP 9802 Station 3 and 5–10 μm long rutile crystals. (b) In K7905-21, barite crystals make up the majority of the barite separation sequential leaching residue in this sample.

[19] The only samples for which 70% or more of the Ba_{excess} is composed of barite are samples from oxic sediments underlying areas of high productivity and low terrigenous input (near the equatorial Pacific and the Polar Front Zone in the Southern Ocean, see samples from JGOFS TT013, TNO57-10 and PS 2498-2). In these sediments, Ba_{excess} (based on an appropriate Ba/Al or Ba/Ti ratio) may indeed be representative of the Ba fraction in the sediments associated with barite [e.g., *Goldberg and Arrhenius*, 1958; *Murray*, 1985; *Murray et al.*, 2000].

[20] The comparison presented here suggests that in most sediments multiple phases of nonbarite sedimentary Ba contribute to the Ba_{excess} value. The effect of including these phases in Ba_{excess} should be considered before attempting paleoproductivity reconstructions. However, this is not the only factor that may introduce potential complications to carbon export estimates using Ba_{excess}. As mentioned previously, the effect of using an inappropriate Ba/Al ratio as a correction for terrigenous Ba may also introduce error. We have evaluated the effect of using different Ba/Al ratios on carbon export estimates by comparing Ba_{excess} calculated with two widely used Ba/Al ratios (Table 3). Ba_{excess} values calculated with the different Ba/Al ratios vary by less than 5% for the majority of the sediments used here, which are mostly from open ocean settings, thus carbon export calculated using these different ratios to derive Ba_{excess} are virtually identical (Table 3). Samples where Ba_{total} is small and Al_{total} is large are exceptions, and the discrepancy between Ba_{excess} calculated with two different ratios is much larger (see samples W7706-44K and INMD 106). These samples demonstrate that the use of an appropriate Ba/Al ratio is especially significant in sediments with high terrigenous input and low barite, in which the terrigenous inventory of Ba is a significant, or even dominant, component of the total Ba inventory, as observed by *Klump et al.* [2000]. In a few samples, Ba_{barite} concentrations exceed the calculated Ba_{excess}, suggesting that the Ba/Al ratio used for correction of terrigenous associated Ba is too high or that there is an additional source of Al (see TNO57-10 and VM-30-41).

[21] In the majority of samples, as indicated previously, Ba_{excess} values are higher than Ba_{barite}, regardless of the Ba/Al ratio used, which could result from either the use of too low a Ba/Al ratio in calculating Ba_{excess} and/or the inclusion of barium from phases other than barite. Ba_{excess} overestimation of Ba_{barite}, however, is too large to be explained entirely by the use of an inappropriately low Ba/Al ratio. Indeed, the Ba/Al ratio required to bring Ba_{excess} down to Ba_{barite} is much higher than is reasonable for terrigenous sources. For example, to lower Ba_{excess} to Ba_{barite}, the Ba/Al ratio for NBP 9802 St. 3, would need to be 0.056, for TT013-113, 0.166 and for PLDS 107, 0.068. We do not feel there is any evidence that these high ratios are more appropriate than the average 0.0075 suggested by *Dymond et al.* [1992]. Thus the discrepancy between Ba_{excess} and Ba_{barite} appears to be mostly a result of the inclusion of nonbarite phases of barium in the calculation of Ba_{excess}.

3.2. *Dymond et al.* [1992] Derived Carbon Export and Measured Ocean Export Fluxes

[22] If applicable, the Ba_{excess} paleoproductivity proxy should result in a robust correlation between measurements of modern ocean carbon export and core top estimates based on the *Dymond et al.* [1992] algorithm. Prior to our study, this exercise had not been completed for any sediment other than site MW (California Current) in the work of *Dymond et al.* [1992]. The more comprehensive comparison presented here, which includes samples from the equatorial Pacific, Atlantic and Southern Ocean (Table 3; Figure 3), offers the first global comparison between present-day carbon export determined from direct measurements and that calculated with the *Dymond et al.* [1992] algorithm as applied to core top sediments. A general correspondence between carbon export (P_{new}), calculated using the *Dymond et al.* [1992] equation for a wide range of core tops, and carbon export determined from water column measurements of primary

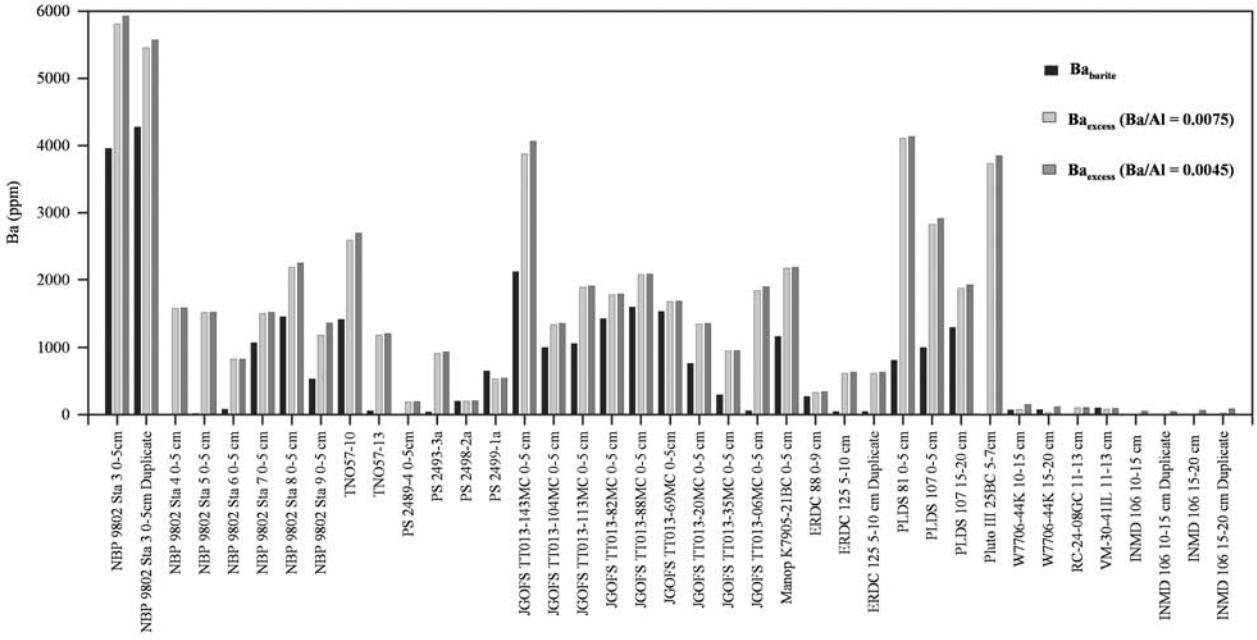

Figure 2. Comparison between Ba_{barite} and Ba_{excess} (calculated with two ratios, Ba/Al of 0.0045 and 0.0075), suggesting considerable Ba exists in phases other than barite and terrigenouse silicates. Ba_{excess} clearly overestimates Ba_{barite} in many samples.

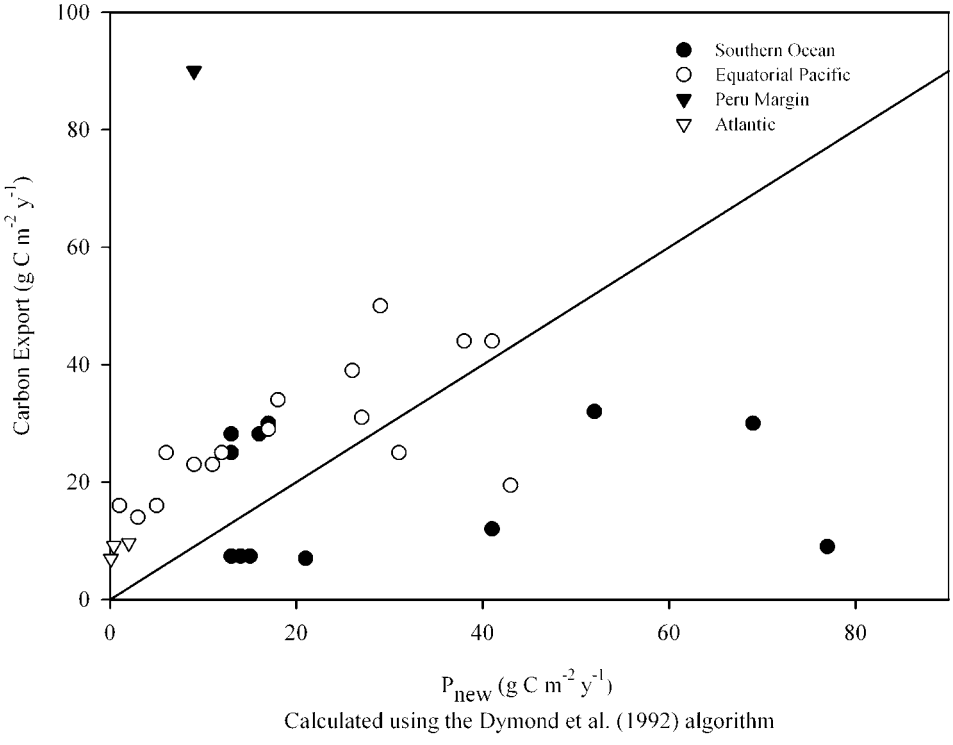

Figure 3. Comparison between carbon export (P_{new}) calculated with the *Dymond et al.* [1992] productivity algorithm from Ba_{excess} (Ba/Al = 0.0075) and the measured carbon export. The line represents a one-to-one relationship between P_{new} and export production. All calculated P_{new} are based on Ba_{excess} values from this study and are found in Table 3, along with carbon export rates.

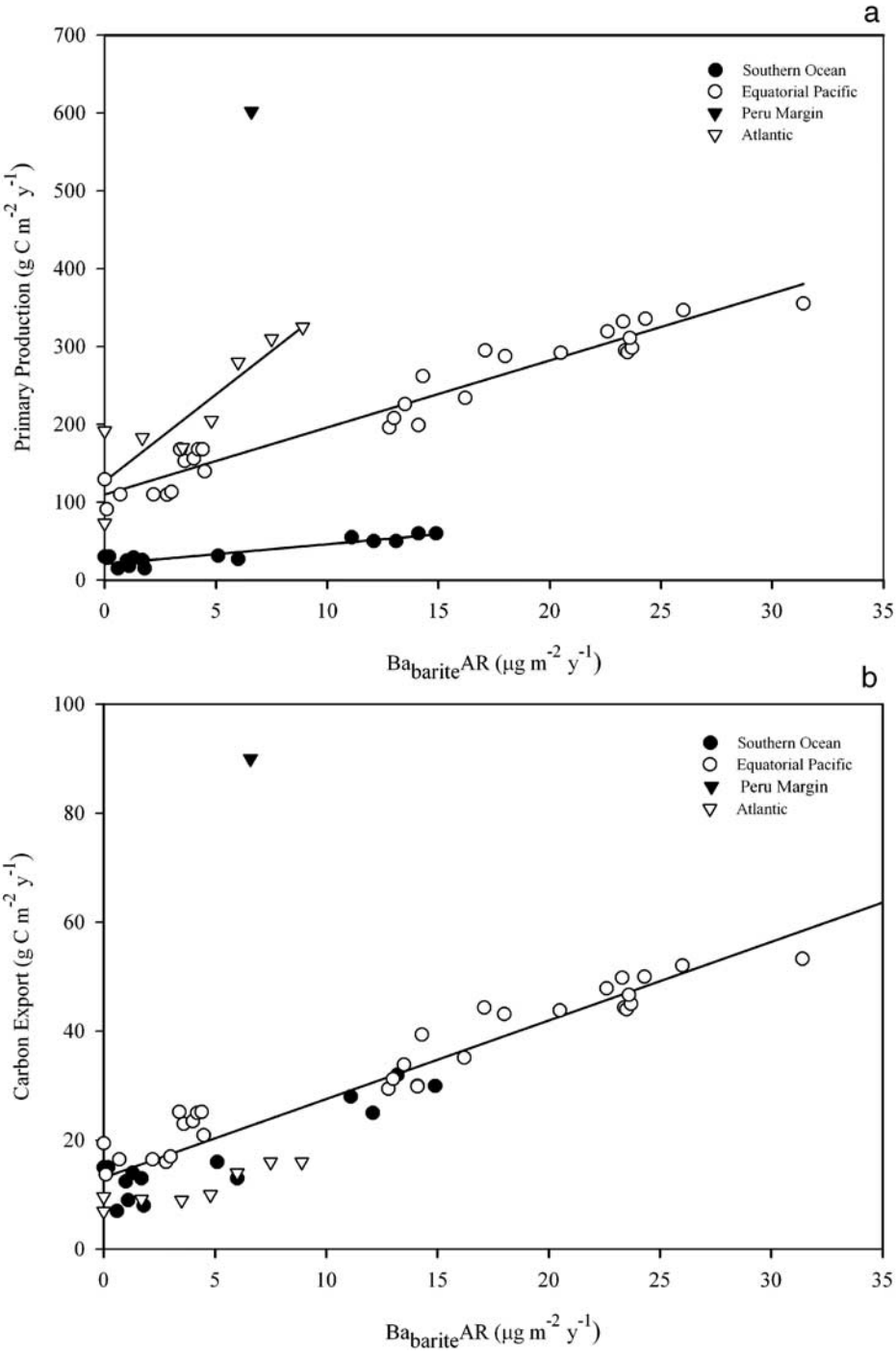

Figure 4. (a) Ba_{barite} accumulation rates (Ba_{barite} AR) in core top sediments plotted against primary productivity in the overlying water column. The figure shows that the relationship between Ba_{barite} and primary productivity is specific to each ocean basin. (b) Ba_{barite} accumulation rates plotted against carbon export calculated from the application of an appropriate f ratio to primary productivity estimates. In addition to samples in Table 3, we included results previously published from sites VNTR01, PLDS 70, 77 and 85 [*Paytan et al.*, 1996], and ERDC 131, PS 2500-7, and TNO57-21 (Paytan, unpublished data).

production and f ratios is observed (Figure 3). Most samples from the equatorial Pacific and Atlantic, however, fall above the 1:1 line, indicating that the calculated carbon export underestimates the measured export. Calculated carbon export values for most samples are within a factor of three of measured export, except where Ba_{excess} is low (INMD 106, RC-24, VM-30 and W7706). Some samples from the Southern Ocean overestimate carbon export, possibly

because the original *Dymond et al.* [1992] algorithm did not include samples from areas with relatively low primary productivity and high export fluxes, such as the Southern Ocean.

3.3. Ba_{barite} Accumulation Rates and Productivity

[23] In contrast to the positive but generally weak relationship between Ba_{excess} in core tops and measured carbon export, as discussed above, Ba_{barite} accumulation exhibits very strong site-specific positive correlations with primary productivity (Figure 4a), with the equatorial Pacific (r^2 = 0.95), Atlantic (r^2 = 0.80) and Southern Ocean (r^2 = 0.85) all exhibiting different regression slopes. Unfortunately, only one sample from the highly productive coastal Peru margin (W7706) was available, so that a relationship between Ba_{barite} and primary production could not be determined for that site. It is not surprising that the correspondence between Ba_{barite} accumulation and primary production is site specific. Barite forms in association with aggregates of decaying organic matter; therefore barite accumulation should be more directly related to the exported fraction of primary production (e.g., carbon export), which varies throughout the ocean.

[24] When primary production is converted to carbon export (new production) using the appropriate f ratio, the site-specific relationships between Ba_{barite} and primary production (Figure 4a) collapse into a single, highly significant ($p < 0.01$) relationship between Ba_{barite} and carbon export flux (P_{new}) (Figure 4b). The only outlier is the sample from the Peru Margin (W7706). A possible explanation for this is that the high productivity measured at present in this region is not representative of the Holocene period represented in the core top sample. It is interesting that the Atlantic samples generally tend to fall below the global regression curve. This may be a result of lower preservation rates of barite in the less Ba-saturated Atlantic seawater [*Monnin et al.*, 1999]. The effect of barite preservation has not been included in the global curve (Figure 4b), but since the Ba concentrations in the deep ocean do not vary much regionally, there is no need to correct for preservation when only regional trends are used (Figure 4a). Alternatively the f ratio used here may be too low and not representative of the Atlantic sites, and a higher ratio would improve the correlation. It must be emphasized that the Ba concentration in seawater is not the only (and not even the most important) variable controlling barite preservation. In particular, sulfate reduction in sediments will result in barite lose [*McManus et al.*, 1998], accordingly the use of barite for reconstruction of carbon export rates is limited to oxic sediments where barite is not remobilized. Despite ignoring the effect of seawater saturation on barite preservation, the global regression for barite accumulation rates and carbon export has an r^2 of 0.81 when the Peru Margin sample (W7706) is included and 0.89 when it is not. This strong correlation suggests that measurements of Ba_{barite} accumulation can be used in the major ocean basins as a proxy for estimating local rates of carbon export. The positive intercepts in Figures 4a and 4b indicate that in low productivity areas barite is not preserved in the sediments, as suggested by *Paytan et al.* [1996].

[25] The excellent agreement between the Ba_{barite} accumulation and the measured carbon export values is surprising considering the assumptions involved and potential errors associated with this calculation. In particular, primary production estimates are based on at most a couple of decades of observation with considerable interannual variability, while core top sediments average signals over several hundred to several thousand years. In addition, errors associated with MAR estimates, f ratio estimates and effects of differential preservation of barite are all included in the relation. Our results indicate that despite its caveats, Ba_{barite} is an excellent proxy for estimating oceanic carbon export, a quantity that is extremely important in understanding the role of the ocean in the global carbon cycle, and hence, climate change.

4. Conclusions

[26] The Ba_{excess} paleoproductivity proxy performs well in some sediments and can be used with careful consideration of the caveats mentioned here (e.g., in sediments with high Ba_{excess} and low terrigenous input). Ba_{excess} incorporates Ba contained in multiple sedimentary phases other than silicates and barite, including organic matter, biogenic SiO_2, $CaCO_3$, and ferromanganese oxyhydroxides [*Dymond et al.*, 1992; *Gingele and Dahmke*, 1994; *Schroeder et al.*, 1997; *McManus et al.*, 1998; *Eagle and Paytan*, 2001]. As found in earlier studies, before applying the Ba_{excess} algorithm, the presence of nonterrigenous Al or Ti must be considered and the appropriate Ba/Al or Ba/Ti ratios applied to remove terrigenous Ba from Ba_{excess}. The comparison between measured carbon export fluxes and the core top fluxes derived the *Dymond et al.* [1992] algorithm demonstrates that Ba_{excess} remains a useful paleoproductivity proxy in some ocean basins, although this algorithm tends to underestimate carbon export.

[27] The correlation between barite accumulation in marine sediments and carbon export in the ocean is very robust. This high correlation is based on sediment core tops and thus takes into account post depositional changes in the particulate Ba pool. The relationship between C_{org} export and Ba_{excess} found in the water column and in sediment traps is very important, and indeed, represents the fundamental basis for the application of Ba or barite for paleoproductivity research. However, a good paleoproductivity proxy, such as barite, should, if at all possible, be based directly upon the sedimentary phase that is directly related to carbon export flux, and exhibit predictable preservation characteristics. However, as with the Ba_{excess} proxy, care must be taken when utilizing barite accumulation to reconstruct past carbon export fluxes. In particular, this proxy may only be applied in oxic sediments and with the underlying assumption that the processes governing barite formation and preservation in the ocean today have also controlled barite accumulation in the past.

[28] **Acknowledgments.** The authors would like to thank the following individuals and core repositories for providing samples: Bobbie Conard at Oregon State University (NSF Grant OCE97-12024); Warren Smith at the Scripps Institute of Oceanography; Robert Anderson at Lamont Doherty Earth Observatory; Dave Hodell at Florida State University; the Bremen Core Repository; and the University of Rhode Island Core Repository. We

also want to thank R. Anderson, Z. Chase, O. Holm-Hansen, F. Chavez, R. Barber and M. Hiscock for sharing with us unpublished data. Robert Jones and Guangchao Li provided valuable assistance with the SEM and ICP analyses. Rick Murray acknowledges support from NSF OCE-9301097 for geochemical studies of the EqPac JGOFS cores. We would like to thank Roger Francois and three anonymous reviewers for helpful comments. Meagan Eagle was partially supported by a fellowship from the American Meteorological Society and the Wright Fund, Stanford University.

References

Arrigo, K. R., D. L. Worthen, A. Schnell, and M. P. Lizotte, Primary production in Southern Ocean waters, *J. Geophys. Res.*, *103*, 587–600, 1998.

Aufdenkampe, A. K., J. J. McCarthy, M. Rodier, C. Navarette, J. Dunne, and J. W. Murray, Estimation of new production in the tropical Pacific, *Global Biogeochem. Cycles*, *15*(1), 101–112, 2001.

Bains, S., R. D. Norris, R. M. Corfield, and K. L. Faul, Termination of global warmth at the Palaeocene/Eocene boundary through productivity feedback, *Nature*, *407*, 171–174, 2000.

Berger, W. H., and J. S. Killingsley, Box cores from the equatorial Pacific: ^{14}C sedimentation rates and benthic mixing, *Mari. Geol.*, *45*, 93–125, 1982.

Bishop, J. K. B., The barite-opal-organic carbon association in oceanic particulate matter, *Nature*, *332*, 341–343, 1988.

Buesseler, K. O., R. T. Barber, M. L. Dickson, M. R. Hiscock, J. K. Moore, and R. N. Sambrotto, The effect of marginal ice-edge dynamics on production and export in the Southern Ocean along 170°W, *Deep Sea Res., Part II*, in press, 2003.

Bonn, W. J., F. X. Gingele, H. Grobe, A. Mackensen, and D. Futterer, Palaeoproductivity at the Antarctic continental margin: opal and barium records for the last 400 ka, *Palaeogeogr. Palaeoclimatol. Palaeoecol.*, *139*, 195–211, 1998.

Chase, Z., Trace elements as regulators (Fe) and recorders (U, Pa, Th, Be) of biological productivity in the ocean, Ph.D. thesis, Columbia Univ., New York, 2001.

Collier, R., and J. M. Edmond, The trace elements geochemistry of marine biogenic particulate matter, *Progr. Oceanogr.*, *13*, 113–199, 1984.

Curry, W. B., and G. P. Lohmann, Reconstructing past particle fluxes in the tropical Atlantic Ocean, *Paleoceanography*, *5*(4), 487–505, 1990.

da Silva, A., A. C. Young, and S. Levitus, *Atlas of Surface Marine Data 1994*, U.S. Dep. of Comm., Washington, D. C., 1994.

Dean, W. E., J. V. Gardner, and D. A. Piper, Inorganic geochemical indicators of glacial-interglacial changes in productivity and anoxia on the California continental margin, *Geochim. Cosmochim. Acta*, *61*, 4507–4518, 1997.

Dehairs, F., R. Chesselet, and J. Jedwab, Discrete suspended particles of barite and the barium cycle in the open ocean, *Earth Planet. Sci.*, *49*, 528–550, 1980.

Dehairs, F., L. Goeyens, N. Stroobants, P. Bernard, C. Goyet, A. Poisson, and R. Chesselet, On suspended barite and the oxygen minimum in the Southern Ocean, *Global Biogeochem. Cycles*, *4*, 85–102, 1990.

DeMaster, D. J., and R. H. Pope, C-14 chronologies, biogenic accumulation rates and sediment mixing coefficients along the equatorial Pacific JGOFS transect (abstract), presented at the Oceanographic Society Fourth Annual Meeting, Oceanogr. Soc., Honolulu, Hawaii, 1994.

Dobson, F. W., and S. D. Smith, Bulk models of solar radiation at sea, *Q. J. R. Meteorol. Soc.*, *114*, 165–182, 1988.

Dymond, J., and R. Collier, Particulate barium fluxes and their relationships to biological productivity, *Deep Sea Res., Part II*, *43*, 1283–1308, 1996.

Dymond, J., E. Suess, and M. Lyle, Barium in deep-sea sediment: A geochemical proxy for paleoproductivity, *Paleoceanography*, *7*, 163–181, 1992.

Eagle, M., and A. Paytan, Phase associations of particulate barium, *Eos Trans. AGU*, *82*(47), Fall Meet. Suppl., abstract PP11A-0459, 2001.

Emerson, S., K. Fischer, C. Reimers, and D. Heggies, Organic carbon dynamics and preservation in deep-sea sediment, *Deep Sea Res., Part II*, *32*, 1–21, 1985.

Francois, R., S. Honjo, S. J. Manganini, and G. E. Ravizza, Biogenic barium fluxes to the deep sea: Implications for paleoproductivity reconstruction, *Global Biogeochem. Cycles*, *9*, 289–303, 1995.

Ganeshram, R., R. Francois, J. Commeau, and S. Brown-Leger, An experimental investigation of barite formation in seawater, *submitted to Geochimica Cosmochimica Acta*, 2002.

Geochemical Ocean Sections Study (GEOSECS), *Atlantic, Pacific and Indian Ocean Expeditions*, vol. 7, *Shorebased Data and Graphics*, Natl. Sci. Found., Washington, D. C., 1987.

Gingele, F., and A. Dahmke, Discrete barite particles and barium as tracers of paleoproductivity in South Atlantic sediments, *Paleoceanography*, *9*, 151–168, 1994.

Goldberg, E. D., and G. O. S. Arrhenius, Chemistry of Pacific pelagic sediments, *Geochim. Cosmochim. Acta*, *13*, 153–212, 1958.

Gregg, W. W., and K. L. Carder, A simple spectral solar irradiance model for cloudless maritime atmospheres, *Limnol. Oceanogr.*, *35*, 1657–1675, 1990.

Hiscock, M. R., J. Marra, W. O. Smith Jr., R. Goericke, C. I. Measures, S. Vink, R. J. Olson, H. M. Sosik, and R. T. Barber, Primary Productivity and its Regulation in the Pacific Sector of the Southern Ocean, *Deep Sea Res., Part II*, in press, 2003.

Kalnay, E., et al., The NCEP/NCAR 40-year reanalysis project, *Bull. Am. Meteorol. Soc.*, *77*, 437–471, 1996.

Kara, A. B., P. A. Rochford, and H. E. Hurlburt, Naval Research Laboratory Mixed Layer Depth (NMLD) climatologies, *NRL Rep. NRL/FR/7330-02-9995*, 26 pp., Nav. Res. Lab., Washington, D. C., 2002.

Klump, J., D. Hebbeln, and G. Wefer, The impact of sediment provenance on barium-based productivity estimates, *Mar. Geol.*, *169*, 259–271, 2000.

Krissek, L. A., K. F. Scheidegger, and L. D. Kulm, Surface sediments of the Peru-Chile continental margin and the Nazca plate, *Geol. Soc. Am. Bull.*, *91*, 321–331, 1980.

McCarthy, J. J., C. Garside, J. L. Nevins, and R. T. Barber, New production along 140 degrees W in the equatorial Pacific during and following the 1992 El Nino event, *Deep Sea Res., Part II*, *43*(4–6), 1065–1093, 1996.

McManus, J., et al., Geochemistry of barium in marine sediments: Implications for its use as a paleoproxy, *Geochim. Cosmochim. Acta*, *62*, 3453–3473, 1998.

Metzler, P. M., P. M. Glibert, S. A. Gaeta, and J. M. Ludlam, New and regenerated production in the South Atlantic off Brazil, *Deep Sea Res., Part I*, *44*(3), 363–384, 1997.

Mix, A. C., W. F. Ruddiman, and A. McIntyre, Late Quaternary paleoceanography of the tropical Atlantic, 1, Spatial variability of annual mean sea-surface temperatures, 0–20,000 years B.P., *Paleoceanography*, *1*, 43–66, 1986.

Monnin, C., C. Jeandel, T. Cattaldo, and F. Dehairs, The marine barite saturation stat of the world's ocean, *Mar. Chem.*, *65*, 253–256, 1999.

Murray, D. W., Spatial and temporal variations in sediment accumulation in the central tropical Pacific, Ph.D. thesis, Oreg. State Univ., Bend, Oreg., 1985.

Murray, R. W., and M. Leinen, Chemical transport to the seafloor of the equatorial Pacific Ocean across a latitudinal transect at 135°W: Tracking sedimentary major, trace, and rare earth element fluxes at the equator and the Intertropical Convergence Zone, *Geochim. Cosmochim. Acta*, *57*, 4141–4163, 1993.

Murray, R. W., and M. Leinen, Scavenged excess Al and its relationship to bulk Ti in biogenic sediment from the central equatorial Pacific Ocean, *Geochm. Cosmochim. Acta*, *60*, 3869–3878, 1996.

Murray, R. W., M. Leinen, and A. R. Isern, Biogenic flux of Al to sediment in the equatorial Pacific Ocean: Evidence for increased productivity during glacial episodes, *Paleoceanography*, *8*, 651–670, 1993.

Murray, R. W., C. Knowlton, M. Leinen, A. C. Mix, and C. H. Polsky, Export production and carbonate dissolution in the central equatorial Pacific Ocean over the past 1 Ma., *Paleoceanography*, *15*, 570–592, 2000.

Nelson, D. M., et al., Vertical budgets for organic carbon and biogenic silica in the Pacific sector of the Southern Ocean, 1996–1998, *Deep Sea Res., Part II*, *49*, 1645–1674, 2002.

Nürnberg, C. C., Bariumfluss und sedimentation im Südatlantik-Hinweise auf produktivitätsänderungen im Quartär, *Rep. 38*, 105 pp., GEOMAR, Kiel, 1995.

Nürnberg, C. C., G. Bohrmann, and M. Schlüter, Barium accumulation in the Atlantic sector of the Southern Ocean: Results from 190,000-year record, *Paleoceanography*, *12*, 594–603, 1997.

Paytan, A., Marine barite: A recorder of oceanic chemistry, productivity and circulation, Ph.D. thesis, Univ. of Calif., San Diego, Calif., 1996.

Paytan, A., and M. Kastner, Benthic Ba fluxes in the central equatorial Pacific, implications for the oceanic Ba cycle, *Earth Planet. Sci.*, *142*, 439–450, 1996.

Paytan, A., M. Kastner, and F. P. Chavez, Glacial to interglacial fluctuations in productivity in the equatorial Pacific as indicated by marine barite, *Science*, *274*, 1355–1357, 1996.

Pena, M. A., W. G. Harrison, and M. R. Lewis, New production in the central equatorial Pacific, *Mar. Ecol. Prog. Ser.*, *80*(2–3), 265–274, 1992.

Rutsch, H. J., A. Mangini, G. Bonai, B. Dittrich-Hannen, P. W. Kubik, M. Suter, and M. Segl, ^{10}Be and Ba concentrations in west African sediments trace productivity in the past, *Earth Planet. Sci.*, *133*, 129–143, 1995.

Schenau, S. J., M. A. Prins, G. J. De Lange, and C. Monnin, Ba accumulation in the Arabian Sea: Controls on barite preservation in marine sediments, *Geochim. Cosmochim. Acta*, *65*, 1545–1556, 2001.

Schmitz, B., Barium, equatorial high productivity, and the northward wandering of the Indian continent, *Paleoceanography*, *2*, 63–77, 1987.

Schroeder, J. O., R. W. Murray, M. Leinen, R. C. Pflaum, and T. R. Janecek, Barium in equatorial Pacific carbonate sediment: Terrigenous, oxide, and biogenic associations, *Paleoceanography*, *12*, 125–146, 1997.

Slutz, R. J., S. J. Lubker, J. D. Hiscox, S. D. Woodruff, R. L. Jenne, P. M. Steurer, and J. D. Elms, *Comprehensive Ocean-Atmosphere Data Set: Release 1*, Clim. Res. Prog., Boulder, Colo., 1985.

Snoeckx, H., and D. K. Rea, Dry bulk density and CaCO3 relationships in upper Quaternary sediments of the eastern equatorial Pacific, *Mar. Geol.*, *120*, 327–333, 1994.

Van Bennekom, A. J., J. H. F. Jarsen, S. J. Der Gaast, J. M. Van Ipeven, and J. Pieters, Aluminum-rich opal: An intermediate in the preservation of biogenic silica in the Zaire (Congo) deep-sea fan, *Deep Sea Res.*, *36*, 173–190, 1989.

Van Capellen, P., S. Dixit, and A. J. van Bennekom, Processes controlling solubility of biogenic silica and pore water build-up of silicic acid in marine sediments, *Mar. Chem.*, *73*, 333–352, 2001.

Wefer, G., E. Suess, W. Balzer, G. Liebezeit, P. J. Muller, C. A. Ungerer, and W. Zenk, Fluxes of biogenic components from sedimentary trap experiments, *Nature*, *299*, 145–147, 1982.

Wollast, R., and L. Chou, The carbon cycle at the ocean margin in the northern Gulf of Biscay, *Deep Sea Res., Part II*, *48*(14–15), 3265–3293, 2001.

K. R. Arrigo and G. van Dijken, Department of Geophysics, Stanford University, Stanford, CA 94305, USA. (arrigo@pangea.stanford.edu; gertvd@stanford.edu)

M. Eagle and A. Paytan, Department of Geological and Environmental Sciences, Stanford University, Stanford, CA 94305-2115, USA. (meagan@intnet.mu; apaytan@pangea.stanford.edu)

R. W. Murray, Department of Earth Sciences, Boston University, Boston, MA 02215, USA. (rickm@bu.edu)